sessing a longer hydrophilic PEG chain and a shorter hydrophobic P(Asp(ADR)) chain circulated longer in blood (Kwon et al., 1993, 1994), accumulated more in tumors (Kwon et al., 1994), and showed greater antitumor activity (Yokoyama et al., 1993). This is a reversed relationship estimated from the CMC phenomenon of block copolymers. This implies that dynamic stability of the polymeric micelles that is defined with a dissociation constant of the micelle structure is more important in vivo than static micelle stability that is defined with CMC values. In this study, at a similar number of the Asp units, the micelles possessing PEG 5000 was found to be more stable than those possessing PEG 12,000 in blood circulation. This fact was opposite to the ADR case. More detailed study is required to elucidate the relationship between in vivo stability and compositions of polymeric micelles by more quantitatively evaluating strength and nature (e.g., degree of contribution of π–π interaction) of interactions utilized for micelle formation and drug incorporation.

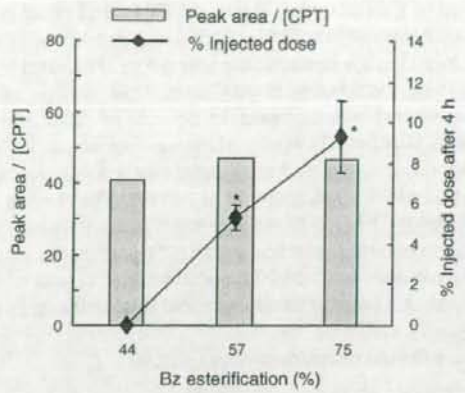

Fig. 3. Effect of esterification of 5-27 Bz on stability of CPT-loaded micelles at a feeding ratio (CPT/polymer) of 0.4 (w/w). The ratio of peak area/[CPT] indicated the incorporation stability of CPT-loaded micelles. Percentage injected dose represents the mean ± S.D., $n = 3$. $^{*}P < 0.05$; compared with 5-27 Bz44.

3.4. Benzyl ester content in micelles

For the ADR-loaded polymeric micelle system, a larger amount of the chemically conjugated ADR (63 mol% with respect to the aspartic acid residue of the block copolymer) provided more stable circulation in blood of the physically entrapped ADR that exhibited targeted anti-tumor activity than a smaller amount case (41 mol%). In the present study, to determine the contribution of esterification to micelle stability, three kinds of 5-27 micelles with different amounts of Bz were prepared. The mean particle sizes of 5-27 Bz44, Bz57 and Bz75 were 275.8, 182.7 and 196.1 nm, respectively. The effect of esterification of 5-27 Bz on the stability of CPT-loaded micelles at a feeding ratio (CPT/polymer) of 0.4 (w/w) was examined by GPC and by measuring the % injected dose in plasma after 4 h (Fig. 3). When the benzyl ester content was increased from 44 to 75%, the stability of polymeric micelles was similar in vitro, but CPT-loaded micelles of 5-27 Bz44 showed poor circulation stability. CPT-loaded micelles were able to maintain stability in vivo on esterification of more than 57% of the polymer. As showing Table 2, PEG–PBLA (Bz100%) micelles were not stable in in vitro. Therefore, stable micelle formulation was obtained when the esterification ratio of Bz was appropriate (57–75%). This finding corresponded well that CPT release rate from the micelles for PEG–PBLA or 5-27 Bz44 was faster than that for 5-27 Bz75, when incubated in PBS at 37 °C (Opanasopit et al., 2004). The result suggested that the contribution of π–π interaction between aromatic groups of CPT molecules could be maintained, when the degree of esterification of Bz was more than 57%.

3.5. Feeding ratio of CPT/polymer in micelle

To investigate the influence of feeding ratio on the micelle characteristics, CPT-loaded polymeric micelles were prepared at the different feeding ratio (0.05, 0.1, 0.2 and 0.4 (w/w)). Fig. 4 shows the entrapment efficiency, mean particle size, and the incorporation and circulation stability of CPT-loaded 5-27 Bz57 polymeric micelles, respectively. Regardless of feeding

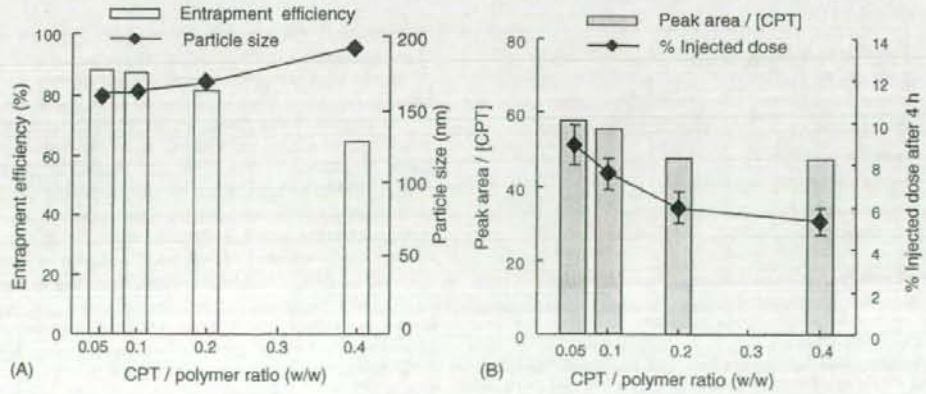

Fig. 4. Effect of feeding ratio (CPT/5-27 Bz57 polymer, w/w) on entrapment efficiency, particle size (A), and the incorporation (peak area/[CPT]) and circulation stability of CPT-loaded micelles (B). Particle size and % injected dose represent the mean ± S.D., $n = 3$.

ratio of CPT/polymer, obtained CPT-loaded micelles showed similar particle size (150–200 nm) and stability of in vitro and in vivo (5–10% injected dose after 4 h). CPT-loaded 5-27 Bz57 micelles were stable in vivo even if the amount of CPT in the polymer was increased. In the case of ADR-loaded polymeric micelles, 21 w/w% ADR was physically incorporated whereas intact ADR, having antitumor activity, accounted for only 5 w/w% (Yokoyama et al., 1999). The feeding ratio of 0.4 (w/w) CPT/polymers corresponds to more than 20 w/w% of CPT in obtained micelles, where CPT was incorporated in the active lactone form (>95%). Therefore, this system will be able to deliver a massive amount of intact drug to the targeted site.

3.6. Plasma concentration–time profiles

As a stable formulation of CPT-loaded micelle was obtained using the polymer with 57–75% Bz esterification at a feeding ratio (CPT/polymer) of 0.4 (w/w), the plasma pharmacokinetics of the CPT-loaded 5-27 Bz63 polymeric micelles was compared with unstable formulations such as 5-27 Bz44 and CPT solution (Fig. 5). CPT-loaded 5-27 Bz63 and 5-27 Bz44 micelles at a feeding ratio (CPT/polymer) of 0.4 (w/w) showed 275.8 ± 14.8 and 276.5 ± 24.8 nm in size, respectively. As expected from Fig. 3, a long-circulation was obvious for the CPT in 5-27 Bz63 compared to 5-27 Bz44 and CPT solution. This finding corresponded with the result of CPT release from polymeric micelles in vitro, showing the slower CPT release from 5-27 Bz75 than 5-27 Bz44 in PBS at 37 °C (Opanasopit et al., 2004). Hydrophilic PEG chains exposed to the aqueous surroundings may prevent the adsorption of blood proteins onto the micelles' surface and from being cleared through RES. In spite of similar particle size, the stable polymeric micelle (Bz63) showed about a 17-fold lower clearance value than the unstable one (Bz44) (Table 4). This finding suggested that the stable incorporation of CPT into micelles by the hydrophobic interaction of intact CPT with inner core of polymeric micelles, e.g., π–π interactions of the benzyl ester, may be important in the circulation stability.

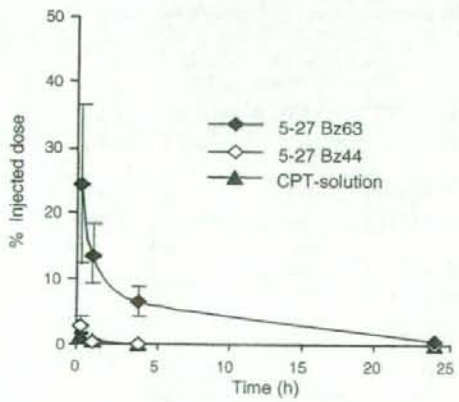

Fig. 5. Plasma concentration–time curves of the CPT-loaded 5-27 Bz (44 or 63) micelles and CPT solution following i.v. administration at a dose of 2.5 mg CPT/kg in ddY mice. The feeding ratio (CPT/polymer) was 0.4 (w/w). Results are given as the mean ± S.D., $n = 3$.

Table 4
Pharmacokinetic parameters after i.v. administration of CPT-loaded 5-27 Bz (44 or 63) micelles in mice at a dose of 2.5 mg/kg

Code	AUC ($\mu g\,h\,ml^{-1}$)	Clearance ($ml\,h^{-1}\,g^{-1}$)	
5-27 Bz63	47.0 ± 2.4	0.053 ± 0.003	**
5-27 Bz44	2.7 ± 0.02	0.91 ± 0.007	

The feeding ratio (CPT/polymer) was 0.4 (w/w). AUC: area under the concentration–time curve from 0 to 24 h. Results are given as the mean±S.D. ($n = 3$).
** $P < 0.01$

4. Conclusion

The stable formulation of CPT-loaded micelles in vivo strongly depended on the amount of benzyl esters and length of the PEG of polymers, more so than in vitro. A stable formulation of CPT-loaded micelles was obtained using PEG-P(Asp) with a PEG of 5000 (MW), 27 Asp units, and 57–75% benzyl esterification. The CPT-loaded micelles are potentially delivered to tumor sites owing to an extended circulation in the blood stream.

Acknowledgments

We are grateful to Ms. C. Kanai, Ms. S. Katayama and Ms. C. Fujita for their technical assistance.

References

Burke, T.G., Staubus, A.E., Mishra, A.K., 1992. Liposomal stabilization of camptothecin's lactone ring. J. Am. Chem. Soc. 114, 8318–8319.
Cortesi, R., Esposito, E., Maietti, A., Menegatti, E., Nastruzzi, C., 1997. Formulation study for the antitumor drug camptothecin: liposomes, micellar solution, and a microemulsion. Int. J. Pharm. 159, 95–103.
Fassberg, J., Stella, V.J., 1992. A kinetic and mechanistic study of the hydrolysis of camptothecin and some analogues. J. Pharm. Sci. 81, 676–684.
Giovanella, B.C., Hinz, H.R., Kozielski, A.J., Stehlin Jr., J.S., Silber, R., Potmesil, M., 1991. Complete growth inhibition of human cancer xenografts in nude mice by treatment with 20-(*S*)-camptothecin. Cancer Res. 51, 3052–3055.
Giovanella, B.C., Stehlin, J.S., Wall, M.E., Wani, M.C., Nicholas, A.W., Liu, L.F., Silber, R., Potmesil, M., 1989. DNA topoisomerase I-targeted chemotherapy of human colon cancer in xenografts. Science 246, 1046–1048.
Hertzberg, R.P., Caranfa, M.J., Hecht, S.M., 1989. On the mechanism of topoisomerase I inhibition by camptothecin: evidence for binding to an enzyme-DNA complex. Biochemistry 28, 4629–4638.
Kang, J., Kumar, V., Yang, D., Chowdhury, P.R., Hohl, R.J., 2002. Cyclodextrin complexation: influence on the solubility, stability, and cytotoxicity of camptothecin, an antineoplastic agent. Eur. J. Pharm. Sci. 15, 163–170.
Kwon, G., Suwa, S., Yokoyama, M., Okano, T., Sakurai, Y., Kataoka, K., 1994. Enhanced tumor accumulation and prolonged circulation times of micelle-forming poly(ethylene oxide-aspartate) block copolymer-adriamycin conjugates. J. Control. Rel. 29, 17–23.
Kwon, G.S., Yokoyama, M., Okano, T., Sakurai, Y., Kataoka, K., 1993. Biodistribution of micelle-forming polymer-drug conjugates. Pharm. Res. 10, 970–974.
Leibler, L., Orland, H., Wheeler, J.C., 1983. Theory of critical micelle concentration for solutions of block copolymers. J. Chem. Phys. 79, 3550–3557.
Maeda, H., 2000. The enhanced permeability and retention (EPR) effect in tumor vasculature. The key role of tumor-selective macromolecular drug targeting. Adv. Enzyme Regul. 41, 189–207.

Maeda, H., Wu, J., Sawa, T., Matsumura, Y., Hori, K., 2000. Tumor vascular permeability and the EPR effect in macromolecular therapeutics: a review. J. Control. Rel. 65, 271–284.

Matsumura, Y., Maeda, H., 1986. A new concept for macromolecular therapeutics in cancer chemotherapy: mechanism of tumoritropic accumulation of proteins and the antitumor agent smancs. Cancer Res. 46, 6387–6392.

Moertel, C.G., Schutt, A.J., Reitemeier, R.J., Hahn, R.G., 1972. Phase II study of camptothecin (NSC-100880) in the treatment of advanced gastrointestinal cancer. Cancer Chemother. Rep. 56, 95–101.

Onishi, H., Machida, Y., Machida, Y., 2003. Antitumor properties of irinotecan-containing nanoparticles prepared using poly(DL-lactic acid) and poly(ethylene glycol)-block-poly(propylene glycol)-block-poly(ethylene glycol). Biol. Pharm. Bull. 26, 116–119.

Opanasopit, P., Yokoyama, M., Watanabe, M., Kawano, K., Maitani, Y., Okano, T., 2004. Block copolymer design for camptothecin incorporation into polymeric micelles for passive tumor targeting. Pharm. Res. 21, 2001–2008.

Shenderova, A., Burke, T.G., Schwendeman, S.P., 1999. The acidic microclimate in poly(lactide-co-glycolide) microspheres stabilizes camptothecins. Pharm. Res. 16, 241–248.

Singer, J.W., Bhatt, R., Tulinsky, J., Buhler, K.R., Heasley, E., Klein, P., de Vries, P., 2001. Water-soluble poly-(L-glutamic acid)-Gly-camptothecin conjugates enhance camptothecin stability and efficacy in vivo. J. Control. Rel. 74, 243–247.

Tong, W., Wang, L., D'Souza, M.J., 2003. Evaluation of PLGA microspheres as delivery system for antitumor agent-camptothecin. Drug Dev. Ind. Pharm. 29, 745–756.

Wall, M.E., Wani, M.C., 1995. Camptothecin and analogs: from discovery to clinic. In: Potmesil, M., Pinedo, H. (Eds.), Camptothecin: New Anticancer Agents. CRC Press, Boca Raton, FL, pp. 21–41.

Wall, M.E., Wani, M.C., Cook, C.E., Palmer, K.H., Mcphail, A.T., Sim, G.A., 1966. Plant antitumor agents. I. The isolation and structure of camptothecin, a novel alkaloidal leukemia and tumor inhibitor from Camptotheca acuminate. J. Am. Chem. Soc. 88, 3888–3890.

Warner, D.L., Burke, T.G., 1997. Simple and versatile high-performance liquid chromatographic method for the simultaneous quantitation of the lactone and carboxylate forms of camptothecin anticancer drugs. J. Chromatogr. B: Biomed. Sci. Appl. 691, 161–171.

Yang, S.C., Lu, L.F., Cai, Y., Zhu, J.B., Liang, B.W., Yang, C.Z., 1999. Body distribution in mice of intravenously injected camptothecin solid lipid nanoparticles and targeting effect on brain. J. Control. Rel. 59, 299–307.

Yokoyama, M., Fukushima, S., Uehara, R., Okamoto, K., Kataoka, K., Sakurai, Y., Okano, T., 1998. Characterization of physical entrapment and chemical conjugation of adriamycin in polymeric micelles and their design for in vivo delivery to a solid tumor. J. Control. Rel. 50, 79–92.

Yokoyama, M., Inoue, S., Kataoka, K., Yui, N., Sakurai, Y., 1987. Preparation of adriamycin-conjugated poly(ethylene glycol)-poly(aspartic acid) block copolymer. A new type of polymeric anticancer agent. Die Makromolekulare Chemie Rapid Commun. 8, 431–435.

Yokoyama, M., Kwon, G.S., Okano, T., Sakurai, Y., Seto, T., Kataoka, K., 1992. Preparation of micelle-forming polymer-drug conjugates. Bioconjug. Chem. 3, 295–301.

Yokoyama, M., Kwon, G.S., Okano, T., Sakurai, Y., Ekimoto, H., Okamoto, K., Mashiba, H., Seto, T., Kataoka, K., 1993. Composition-dependent in vivo antitumor activity of adriamycin-conjugated polymeric micelle against murine colon adenocarcinoma 26. Drug Del. 4, 11–19.

Yokoyama, M., Kwon, G.S., Okano, T., Sakurai, Y., Naito, M., Kataoka, K., 1994. Influencing factors on in vitro micelle stability of adriamycin-block copolymer conjugates. J. Control. Rel. 28, 59–65.

Yokoyama, M., Miyauchi, M., Yamada, N., Okano, T., Sakurai, Y., Kataoka, K., Inoue, S., 1990. Characterization and anticancer activity of the micelle-forming polymeric anticancer drug adriamycin-conjugated poly(ethylene glycol)–poly(aspartic acid) block copolymer. Cancer Res. 50, 1693–1700.

Yokoyama, M., Okano, T., Sakurai, Y., Ekimoto, H., Shibazaki, C., Kataoka, K., 1991. Toxicity and antitumor activity against solid tumors of micelle-forming polymeric anticancer drug and its extremely long circulation in blood. Cancer Res. 51, 3229–3236.

Yokoyama, M., Okano, T., Sakurai, Y., Fukushima, S., Okamoto, K., Kataoka, K., 1999. Selective delivery of adriamycin to a solid tumor using a polymeric micelle carrier system. J. Drug Target. 7, 171–186.

Yokoyama, M., Opanasopit, P., Okano, T., Kawano, K., Maitani, Y., 2004. Polymer design and incorporation methods for polymeric micelle carrier system containing water-insoluble anti-cancer agent camptothecin. J. Drug Target., 373–384.

Zamai, M., VandeVen, M., Farao, M., Gratton, E., Ghiglieri, A., Castelli, M.G., Fontana, E., D'Argy, R., Fiorino, A., Pesenti, E., Suarato, A., Caiolfa, V.R., 2003. Camptothecin poly[*n*-(2-hydroxypropyl) methacrylamide] copolymers in antitopoisomerase-I tumor therapy: intratumor release and antitumor efficacy. Mol. Cancer Ther. 2, 29–40.

Available online at www.sciencedirect.com
SCIENCE DIRECT
Journal of Controlled Release 112 (2006) 329–332
journal of controlled release
www.elsevier.com/locate/jconrel

Enhanced antitumor effect of camptothecin loaded in long-circulating polymeric micelles

Kumi Kawano [a], Masato Watanabe [a], Tatsuhiro Yamamoto [b], Masayuki Yokoyama [b], Praneet Opanasopit [c], Teruo Okano [c], Yoshie Maitani [a,*]

[a] Institute of Medicinal Chemistry, Hoshi University, 2-4-41 Ebara, Shinagawa-ku, Tokyo 142-8501, Japan
[b] Kanagawa Academy of Science and Technology, KSP East 404, Sakado 3-2-1, Takatsu-ku, Kawasaki-shi, Kanagawa 213-0012, Japan
[c] Institute of Advanced Biomedical Engineering and Science, Tokyo Women's Medical University, Kawada-cho 8-1, Shinjuku-ku, Tokyo 162-8666, Japan

Received 18 October 2005; accepted 20 March 2006
Available online 27 March 2006

Abstract

A water-insoluble antitumor agent, camptothecin (CPT) was successfully incorporated into polymeric micelles formed from poly(ethylene glycol)-poly(benzyl aspartate) block copolymers (CPT-loaded polymeric micelles). Antitumor effects and biodistribution of CPT-loaded micelles were evaluated in mice subcutaneously transplanted by colon 26 tumor cells. Tumor growth was significantly inhibited after a single i.v. injection of CPT-loaded polymeric micelles at doses of either 15 or 30 mg/kg. Efficacy of a single high-dose injection was comparable to low dose multiple injections. CPT loaded in polymeric micelles showed prolonged blood circulation and higher accumulation in tumors compared with CPT in solution. Polymeric micelle systems offer a stable and effective platform for cancer chemotherapy with CPT.

Keywords: Camptothecin; Polymeric micelle; Antitumor effect; Biodistribution; Colon 26 tumor

1. Introduction

In cancer chemotherapy, the usage of anticancer drugs has been limited by their toxic side-effects in normal organs. Anticancer drug carriers, such as liposomes, microspheres and polymeric systems, have been developed to target and improve their efficacy toward malignant cells, and to reduce toxicity. Long-circulating carriers with nanoscopic dimensions in the bloodstream can passively deliver chemotherapeutic agents to tumor sites via an enhanced permeability and retention effect (EPR effect) [1,2].

Polymeric micelles are prepared from block copolymers possessing both hydrophilic and hydrophobic chains, and they have received much attention in drug delivery research. Their innate characteristics for drug targeting include solubilization of hydrophobic molecules, small particle size, high structural stability, extended drug release, and prevention of rapid clearance by the reticuloendothelial system. Anticancer drug targeting using polymeric micelles was first employed in enhancing the in vivo anticancer activity of doxorubicin [3,4]. Such systems have now been applied to other anticancer drugs, such as paclitaxel [5], cisplatin [6], methotrexate [7] and KRN 5500 [8].

Camptothecin (CPT), a plant alkaloid extracted from *Camptotheca acuminate*, acts as a potent antitumor agent by inhibiting the nuclear enzyme topoisomerase I. CPT inhibits the growth of a wide range of tumors [9,10]. However, the major drawbacks of the drug have always been water insolubility and lactone instability. The lactone ring in CPT plays an important role in the drug's biological activity but it exists in a pH-dependent equilibrium with an open ring carboxylate form (Fig. 1(A)). The lactone ring opens at physiological pH or above, making this drug much less active and highly toxic (such as myelosuppression, haemorrhagic cystitis and diarrhea), and precludes its clinical use.

In our previous study, CPT was successfully incorporated in poly(ethylene glycol)-poly(L-aspartate ester) block copolymer micelles with high incorporation efficiency by optimizing its preparation method and copolymer structure [11,12]. Polymers exhibiting 60–70% benzyl esterification of the aspartate chain yielded micelles that were stable in blood plasma [13]. In this report, the antitumor effects and biodistribution of CPT-loaded polymeric micelles were evaluated in mice bearing colon

* Corresponding author. Tel./fax: +81 3 5498 5048.
E-mail address: yoshie@hoshi.ac.jp (Y. Maitani).

0168-3659/$ - see front matter © 2006 Elsevier B.V. All rights reserved.
doi:10.1016/j.jconrel.2006.03.012

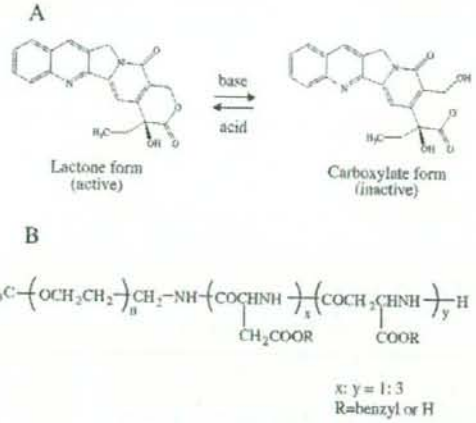

Fig. 1. pH-dependent equilibrium of camptothecin (A) and chemical structure of block copolymer (PEG-P(Asp(Bz-70))) (B).

26 solid tumors. Polymeric micelles loaded with CPT prolonged its blood circulation time and enhanced its antitumor effect due to tumor accumulation by the EPR effect.

2. Materials and methods

2.1. Preparation of CPT-loaded polymeric micelles

Poly(ethylene glycol)-poly(benzyl aspartate-70) block copolymer (PEG-P(Asp(Bz-70))) was synthesized by benzyl-esterification of poly(ethylene glycol)-poly(aspartic acid) as described previously [11]. PEG-P(Asp(Bz-70)) was composed of the poly(ethylene glycol) (PEG) block of molecular weight of 5000 determined by gel-permeation chromatography, and the p(Asp) block possessing 25 units of the aspartic acid residues on average determined by ^{1}H NMR spectroscopy. Seventy percent of the aspartic acid residue was esterified with benzyl group determined by ^{1}H NMR spectroscopy (Fig. 1(B)). From these three values, the molecular weight of PEG-P(Asp(Bz-70)) was calculated to be 9700. (s)-(+)-Camptothecin (CPT, Aldrich Chem. Co.) was incorporated into polymeric micelles by an evaporation method as reported previously [12], using 2 mg of CPT and 5 mg of PEG-P(Asp(Bz-70)). CPT incorporation efficiency in micelle to the drug in preparation was 63%. The average particle size was 191.8±12.7 nm, measured by dynamic light scattering particle size analyzer (ELS-800, Otsuka Electronics, Osaka, Japan).

2.2. Antitumor activity

Antitumor activity of CPT-loaded polymeric micelles was evaluated with mouse bearing colon adenocarcinoma 26. The animal experiments were conducted in accordance with the Guiding Principles for the Care and Use of Laboratory Animals of Hoshi University. Colon 26 cells (1×10^4 cells/0.1 ml) were transplanted into CDF_1 female mice (5 weeks old, Sankyo Labo Service Corporation, Tokyo, Japan) subcutaneously, and drug injection was started when tumor volume reached approximately 100 mm^3. Drug was injected into a tail vein once or three times at a three day interval. CPT solution was prepared by dissolving CPT (13 mg) in 50 ml of polyethylene glycol 400, propylene glycol and polysorbate 80 (40:50:2, volume ratio) [14]. Tumor volume and body weight were measured for individual animals. Tumor volume was calculated as follows; volume$=\pi/6\times LW^2$, where L is the long diameter and W is the short diameter. Percentage of tumor growth inhibition (T/C%) was calculated from relative tumor volume at day 8, following the equation: T/C%$=100\times$(mean relative tumor volume of treated group)/(mean relative tumor volume of control group).

2.3. CPT biodistribution in tumor bearing mice

CPT biodistribution was evaluated in CDF_1 female mice (5 weeks old) subcutaneously transplanted by colon 26 cells (1×10^4 cells/0.1 ml) after tumor volume reached approximately 100 mm^3. CPT-loaded micelles and CPT solution were intravenously administered via lateral tail veins at a dose of 2.5 mg/kg. Twenty-four hours after injection, blood was collected with heparinized syringe and centrifuged to obtain the plasma. The tumor and major tissues were excised and homogenized in phosphate buffered saline (pH 7.4). For the determination of CPT, an aliquot of plasma or the tissue homogenate was acidified with the aqueous phosphoric acid (0.15 M) and then CPT was extracted with chloroform:methanol (4:1 volume ratio). After centrifugation of the mixture, 25 μl of the chloroform:methanol layer was directly analyzed by the HPLC system (Shimadzu Corp., Japan), using a Tosoh TSK-gel ODS-80Ts column (150×4.6 mm I.D., Tosoh Corp., Japan) and a fluorescence detector (excitation: 369 nm, emission: 426 nm). The mobile phase was composed of 23:77 (v/v) acetonitrile-triethylamine acetate buffer (1% (v/v) adjusted to pH 5.5 with glacial acetic acid) at a flow rate 1.0 ml/min [15]. Standard curve with concentrations ranging from 25 ng/ml to 1.0 μg/ml of the drug exhibited good linearity with a correlation coefficient of 0.999.

3. Results and discussion

3.1. Antitumor effect of CPT-loaded polymeric micelles in colon 26 solid tumors

Antitumor effect of CPT-loaded polymeric micelles was evaluated in mice bearing colon 26 solid tumors (Fig. 2). In a preliminary study, murine weight loss was over 20% (three days after injection) and it took two days to recover from a single i.v. administration of 40 mg/kg CPT-loaded polymeric micelles to normal CDF_1 mouse (data not shown). This result suggested that 30 mg/kg would be the maximum dose for murine cancer treatment. The dose of CPT solution (1.5 mg/kg) was decided by its solubility (0.26 mg/ml) in the solvent used and tolerable body weight loss for treatment. Treatment with CPT solution showed tumor growth inhibition (T/C%) of 49.6% at day 8, whereas polymeric micelles treated at either 15 or 30 mg/kg of CPT were 27.5% and 18.5%, respectively (Fig. 2(A)). Furthermore, these polymeric preparations significantly inhibited tumor growth at

day 8 compared with control ($P<0.01$) without significant adverse effects, such as weight loss ($P>0.05$) (Fig. 2(B)).

When the total CPT dose was fixed at 30 mg/kg, a single i.v. injection of CPT-loaded polymeric micelles exhibited comparable inhibition of tumor growth to a triple injection at a dose of 10 mg/kg/day (T/C% of 42.1%) (Fig. 2 (C)). Cytotoxicity of CPT and other topoisomerase I inhibitors is S-phase specific and in vivo studies have suggested that multiple administration of CPT-derivatives were effective against tumors [16]. CPT conjugated with poly(L-glutamic acid) (PG-CPT) or *N*-(2-hydroxypropyl) methacrylamide (HPMA-CPT) needed frequent administration in order to be effective, even though enhanced accumulation was observed in the tumor [17–19]. Furthermore, at equivalent drug levels, repeated administration (40 mg/kg × 4, 4 day interval) of PG-CPT was more efficacious than a single bolus (160 mg/kg) [17]. This discrepancy may be due to a difference in the rate of release of free CPT from the polymeric carriers. Although CPT has been shown to release slowly from PG-CPT and HPMA-CPT [17,19], CPT-loaded polymeric micelles quickly shed nearly half of its load within 24 h, despite retardation by highly benzyl esterified polymer [12]. These findings suggest that the rapid bioavailability of free CPT from the polymeric micelles, relative to other polymeric carriers, may indeed improve antitumor activity subsequent to the passive accumulation of polymeric carriers in the tumor tissue.

3.2. Tumor accumulation of CPT-loaded polymeric micelles

The biodistribution profiles of CPT-loaded polymeric micelles and CPT solution were determined 24 h after i.v. injection of 2.5 mg/kg into mice bearing colon 26 tumor (Fig. 3). Blood

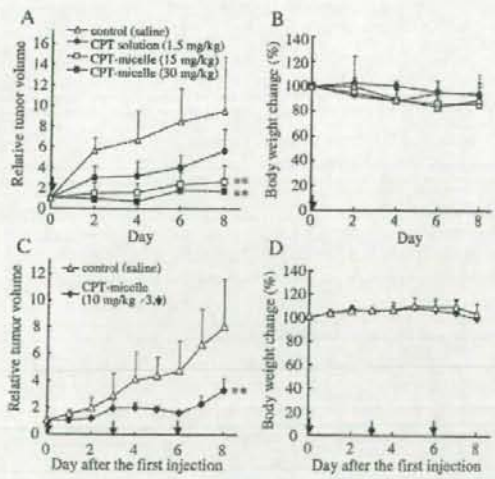

Fig. 2. Antitumor activity (A, C) and body weight change (B, D) after a single (A, B) and a triple (C, D) injection of CPT-loaded polymeric micelles in mice bearing colon 26 tumor. Arrows indicate the day of drug injections. Tumor volumes are plotted in ratios to the initial volume at day 0. Each value represents the mean ± S.D. ($n=4$–5). **: $P<0.01$, compared with control at day 8 (Scheffe's F-test).

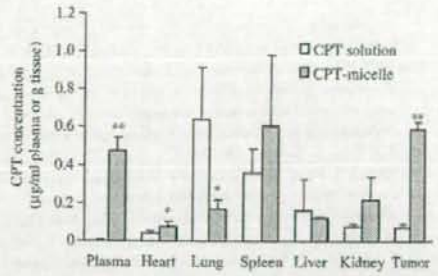

Fig. 3. CPT biodistribution in mice bearing colon 26 tumor 24 h after i.v. injection of CPT-loaded polymeric micelles and CPT solution at a dose of 2.5 mg/kg. Each value represents the mean ± S.D. ($n=3$). *: $P<0.05$, **: $P<0.01$, compared with CPT solution (Students' t-test).

plasma levels of CPT-loaded micelles (1.1% of injected dose) were approximately 150 times higher than CPT solution. Tumor accumulation of CPT-loaded polymeric micelles (approximately 1.3% of injected dose per g tissue) was nearly 8 times higher than CPT solution. Elevated pulmonary CPT levels by CPT solution may be due to embolization of lung capillaries arising from drug precipitation [14].

The pharmacokinetic (area under the plasma concentration–time curve, AUC) profile of CPT-loaded polymeric micelles was approximately 17 times higher than CPT solution when administered at a dose of 2.5 mg/kg in ddY mice [13]. Drug carriers with a prolonged circulation time are able to increase their accumulation in tumor tissues by the EPR effect and, consequently, improve antitumor activity. Furthermore, polymeric micelles could maintain CPT lactone form even in the presence of serum [12]. These characteristics suggest that polymeric micelles possess the ability to deliver large amounts of CPT, in its most active lactone form, to the tumor site by passive targeting with a long-circulating carrier.

4. Conclusion

Polymeric micelles increased the antitumor effects of camptothecin (CPT) in mice subcutaneously transplanted with a colon 26 tumor. The observed therapeutic efficacy of micelles is probably related to the extended circulation time. Passive accumulation of this preparation in tumor sites induced a similar level of significant tumor regression, whether from a single bolus of 30 mg/kg CPT or three repeated doses of 10 mg/kg. Polymeric micelle systems offer a stable and effective platform for cancer chemotherapy with camptothecin.

References

[1] Y. Matsumura, H. Maeda, A new concept for macromolecular therapeutics in cancer chemotherapy: mechanism of tumoritropic accumulation of proteins and the antitumor agent smancs, Cancer Res. 46 (1986) 6387–6392.
[2] H. Maeda, The enhanced permeability and retention (EPR) effect in tumor vasculature: the key role of tumor-selective macromolecular drug targeting, Adv. Enzyme Regul. 41 (2000) 189–207.
[3] M. Yokoyama, T. Okano, Y. Sakurai, H. Ekimoto, C. Shibazaki, K. Kataoka, Toxicity and antitumor activity against solid tumors of

micelle-forming polymeric anticancer drug and its extremely long circulation in blood, Cancer Res. 51 (1991) 3229–3236.
[4] M. Yokoyama, S. Fukushima, R. Uehara, K. Okamoto, K. Kataoka, Y. Sakurai, T. Okano, Characterization of physical entrapment and chemical conjugation of adriamycin in polymeric micelles and their design for in vivo delivery to a solid tumor, J. Control. Release 50 (1998) 79–92.
[5] T.Y. Kim, D.W. Kim, J.Y. Chung, S.G. Shin, S.C. Kim, D.S. Heo, N.K. Kim, Y.J. Bang, Phase I and pharmacokinetic study of Genexol-PM, a cremophor-free, polymeric micelle-formulated paclitaxel, in patients with advanced malignancies, Clin. Cancer Res. 10 (2004) 3708–3716.
[6] N. Nishiyama, S. Okazaki, H. Cabral, M. Miyamoto, Y. Kato, Y. Sugiyama, K. Nishio, Y. Matsumura, K. Kataoka, Novel cisplatin-incorporated polymeric micelles can eradicate solid tumors in mice, Cancer Res. 63 (2003) 8977–8983.
[7] Y. Li, G.S. Kwon, Methotrexate esters of poly(ethylene oxide)-block-poly (2-hydroxyethyl-L-aspartamide). Part I: Effects of the level of methotrexate conjugation on the stability of micelles and on drug release, Pharm. Res. 17 (2000) 607–611.
[8] M. Yokoyama, A. Satoh, Y. Sakurai, T. Okano, Y. Matsumura, T. Kakizoe, K. Kataoka, Incorporation of water-insoluble anticancer drug into polymeric micelles and control of their particle size, J. Control. Release 55 (1998) 219–229.
[9] B.C. Giovanella, H.R. Hinz, A.J. Kozielski, J.S. Stehlin Jr., R. Silber, M. Potmesil, Complete growth inhibition of human cancer xenografts in nude mice by treatment with 20-(S)-camptothecin, Cancer Res. 51 (1991) 3052–3055.
[10] B.C. Giovanella, J.S. Stehlin, M.E. Wall, M.C. Wani, A.W. Nicholas, L.F. Liu, R. Silber, M. Potmesil, DNA topoisomerase I-targeted chemotherapy of human colon cancer in xenografts, Science 246 (1989) 1046–1048.
[11] M. Yokoyama, P. Opanasopit, T. Okano, K. Kawano, Y. Maitani, Polymer design and incorporation methods for polymeric micelle carrier system containing water-insoluble anti-cancer agent camptothecin, J. Drug Target. (2004) 373–384.
[12] P. Opanasopit, M. Yokoyama, M. Watanabe, K. Kawano, Y. Maitani, T. Okano, Block copolymer design for camptothecin incorporation into polymeric micelles for passive tumor targeting, Pharm. Res. 21 (2004) 2001–2008.
[13] M. Watanabe, K. Kawano, M. Yokoyama, P. Opanasopit, T. Okano, Y. Maitani, Preparation of camptothecin-loaded polymeric micelles and evaluation of their incorporation and circulation stability, Int. J. Pharm. 308 (2006) 183–189.
[14] S.C. Yang, L.F. Lu, Y. Cai, J.B. Zhu, B.W. Liang, C.Z. Yang, Body distribution in mice of intravenously injected camptothecin solid lipid nanoparticles and targeting effect on brain, J. Control. Release 59 (1999) 299–307.
[15] D.L. Warner, T.G. Burke, Simple and versatile high-performance liquid chromatographic method for the simultaneous quantitation of the lactone and carboxylate forms of camptothecin anticancer drugs, J. Chromatogr., B, Biomed. Sci. Appl. 691 (1997) 161–171.
[16] J. O'Leary, F.M. Muggia, Camptothecins: a review of their development and schedules of administration, Eur. J. Cancer 34 (1998) 1500–1508.
[17] Y. Zou, Q.P. Wu, W. Tansey, D. Chow, M.C. Hung, C. Charnsangavej, S. Wallace, C. Li, Effectiveness of water soluble poly(L-glutamic acid)-camptothecin conjugate against resistant human lung cancer xenografted in nude mice, Int. J. Oncol. 18 (2001) 331–336.
[18] V.R. Caiolfa, M. Zamai, A. Fiorino, E. Frigerio, C. Pellizzoni, R. d'Argy, A. Ghiglieri, M.G. Castelli, M. Farao, E. Pesenti, M. Gigli, F. Angelucci, A. Suarato, Polymer-bound camptothecin: initial biodistribution and antitumour activity studies, J. Control. Release 65 (2000) 105–119.
[19] M. Zamai, M. VandeVen, M. Farao, E. Gratton, A. Ghiglieri, M.G. Castelli, E. Fontana, R. D'Argy, A. Fiorino, E. Pesenti, A. Suarato, V.R. Caiolfa, Camptothecin poly[*n*-(2-hydroxypropyl) methacrylamide] copolymers in antitopoisomerase-I tumor therapy: intratumor release and antitumor efficacy, Mol. Cancer Ther. 2 (2003) 29–40.

A novel synthetic tissue-adhesive hydrogel using a crosslinkable polymeric micelle

Yoshihiko Murakami,[1] Masayuki Yokoyama,[1] Teruo Okano,[2] Hiroshi Nishida,[3] Yasuko Tomizawa,[3] Masahiro Endo,[3] Hiromi Kurosawa[3]

[1]*Yokoyama Nano-Medical Polymer Project, Kanagawa Academy of Science and Technology (KAST), KSP East 404, Sakado 3-2-1, Takatsu, Kawasaki, Kanagawa 213-0012, Japan*

[2]*Institute of Advanced Biomedical Engineering and Science, Tokyo Women's Medical University, 8-1 Kawada-cho, Shinjuku-ku, Tokyo 162-8666, Japan*

[3]*Department of Cardiovascular Surgery, The Heart Institute of Japan, Tokyo Women's Medical University, 8-1 Kawada-cho, Shinjuku, Tokyo 162-8666, Japan*

Received 20 February 2006; revised 17 March 2006; accepted 3 May 2006
Published online 29 September 2006 in Wiley InterScience (www.interscience.wiley.com). DOI: 10.1002/jbm.a.30911

Abstract: We prepared a novel tissue-adhesive hydrogel by using a polymeric micelle consisting of an aldehyde-terminated poly(ethylene glycol)–poly(D,L-lactide) (PEG–PLA) block polymer. A Schiff base is chemically formed between the amino groups in a polyallylamine and the aldehyde groups on the surface of polymeric micelles. The hydrogel was formed in ~2 s when the polymeric micelle solution and polyallylamine solution are mixed *in vitro*. The hydrogel was rapidly formed *in vivo*, and it adhered to a tissue surface. Our novel tissue-adhesive hydrogel creates no risk of infectious contaminations, because it consists of only synthetic materials. Further, PEG and PLA are known to be biocompatible and noncytotoxic. The results obtained in the present study show that a hydrogel prepared by the formation of a Schiff base between aldehyde and amine groups will potentially address the need for novel tissue-adhesive materials. © 2006 Wiley Periodicals, Inc. J Biomed Mater Res 80A: 421–427, 2007

Key words: tissue-adhesive hydrogel; polymeric micelle; block polymer; polyethylene glycol; polylactide

INTRODUCTION

Tissue-adhesive materials are clinically used for local hemostasis in surgery and for stopping body fluid and air leaks that may be resistant to conventional suture or stapling techniques. In the past few decades, several tissue-adhesive formulations have been developed. These include fibrin glues,[1,2] collagen sheets with fibrin glues,[3] fibrillar collagen,[4] collagen with citric acid derivative,[5] gelatin with resorcin and formalin (GRF glue™),[6] albumin with glutaraldehyde,[7] cyanoacrylate,[8] and synthetic polymers.[9–12] However, these materials have a number of disadvantages and need to be improved for clinical use.

Fibrin-based glues have been widely used in a variety of surgical procedures and are designed to mimic the physiology of the final steps of the blood coagulation cascade. However, there is a risk of infectious contaminations when these glues are used. Collagen and gelatin are not suitable as tissue-contacting materials owing to the same risk factor, although they are known to possess beneficial characteristics—high tensile strength, absorbability in the body, and good cell compatibility. A systemic allergic reaction was reported when collagen-based hemostat was used in a laparoscopic cholecystectomy.[13] Furthermore, the glues that contain these aldehydes as crosslinkers are highly cytotoxic, because aldehydes with low molecular weights (such as formaldehyde and glutaraldehyde) deeply penetrate tissues owing to their high diffusive characteristics.

Synthetic glues have been actively developed because they do not possess the risk of infectious contaminations. Cyanoacrylate is comparable to fibrin glues, but it offers additional benefits such as a relatively high bonding strength and no risk of infectious contaminations. However, its cytotoxicity and lack of biodegradability restrict its use. On the other hand, synthetic polymer-based glues have beeneasily syn-

Correspondence to: M. Yokoyama; e-mail: masajun@ksp.or.jp
Contract grant sponsor: Ministry of Education, Culture, Sports, Science and Technology of Japan

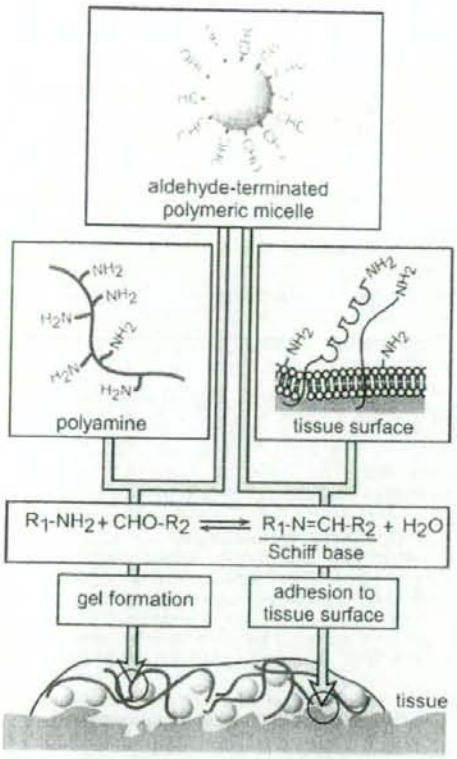

Figure 1. Novel synthetic tissue-adhesive hydrogel that uses a crosslinkable polymeric micelle.

thesized with a molecular design that controls their absorbability, biodegradability, and reactivity, thus making them promising biomaterials. They are polymerized by using photoreactive[9,10] or reactive[11,12] monomers. However, photoactivation makes application of the glue quite difficult and nearly impossible in case of a hemorrhage.

We propose a novel synthetic tissue-adhesive hydrogel that uses a crosslinkable polymeric micelle (Fig. 1). A Schiff base is chemically formed between the amino groups in a polyamine (e.g. polyallylamine) and the aldehyde groups on the surface of a polymeric micelle. A polymeric micelle is a macromolecular spherical particle (molecular weight: ca. 3000–4000 kDa) that is formed from block or grafted polymers in which the hydrophilic and hydrophobic blocks are combined. PEG is known to be biocompatible, because the interaction between PEG and cells is quite low. Actually, the poly(ethylene glycol) (PEG)-based hydrophilic blocks form the shell that helps the micelle to stay unrecognized during blood circulation in drug delivery systems.[14] We can easily transform the micelle into a highly reactive crosslinker by using aldehyde-terminated block polymers. This highly reactive crosslinker may give a fast gelation property to the polymeric micelle-based glue, which is an important property for hemostasis. Owing to these properties, a polymeric micelle can be used as a macromolecular and biocompatible crosslinker in our novel hydrogel. The resulting hydrogel can be expected to adhere to a tissue because of the Schiff base formation between the aldehyde groups on the surface of a polymeric micelle and the amino groups that are present on the tissue surface (e.g. primary amino groups of cell adhesion molecules and lipids).

In the present article, we describe the preparation of a novel hydrogel, the effect that the properties of polymer solutions have on both the hydrogel strength and the gelation time, and the tissue-adhesive properties of the hydrogel to the peritoneum of mice.

MATERIALS AND METHODS

Materials

An acetal-terminated PEG–poly(D,L-lactide) (PEG–PLA) block polymer (**1**, Fig. 2) was synthesized according to a reference.[15] We obtained acetal-terminated PEG–PLA by employing anionic ring-opening polymerization from ethylene oxide and D,L-lactide in tetrahydrofuran. After the reaction, the block polymer was precipitated into cold 2-propanol and lyophilized in benzene. The number-average molecular weights of the acetal-terminated block polymer was 9470 (PEG and PLA units were 5310 and 4010, which were

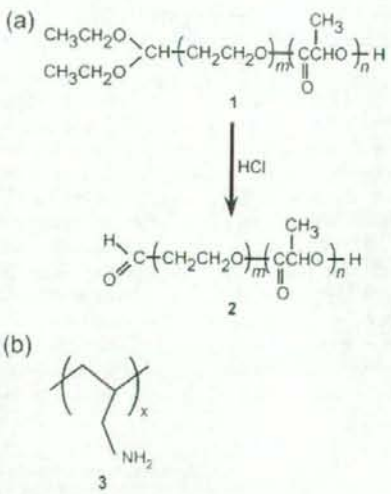

Figure 2. Molecular structure of the polymers, (a) acetal-terminated poly(ethylene glycol-*block*-DL-lactide) and (b) polyallylamine, used in this study.

determined on the basis of a gel permeation chromatography and ^{1}H NMR, respectively). ^{1}H NMR also showed that the acetal group was introduced to 92.6% of the terminus of the polymer. Polyallylamine (3) hydrochloride with average molecular weights of 5000, 15,000, 60,000, and 150,000 were generously provided by Nitto Boseki (Japan) and were used as a polyamine component. All the other reagents were of analytical grade and were used without further purification.

Preparation of an aldehyde-terminated polymeric micelle

Two-types of polymeric micelles were prepared. One consisted of aldehyde (100 w/w%)-terminated PEG–PLA (2) and the other consisted of aldehyde (10 w/w%)/acetal (90 w/w%)-terminated PEG–PLA. We dissolved the acetal-terminated PEG–PLA in *N,N*-dimethylacetamide, and then performed dialysis against water by using a Spectra/Por7 dialysis membrane (molecular weight cut-off: 1 kDa; Spectrum, Houston, TX) for 24 h. We stirred the polymeric micelle solution at pH 2 for 2 h after adding HCl to convert the acetal group into the aldehyde group on the surface of the micelle. To stop the reaction, we adjusted the solution to pH 5 by adding NaOH. The polymeric micelle that consisted of only aldehyde-terminated PEG–PLA was finally obtained through dialysis against water for 24 h, which made possible the removal of the salt. We also prepared the polymeric micelle that consisted of aldehyde (10 w/w%)/acetal (90 w/w%)-terminated PEG–PLA by mixing both the lyophilized polymeric micelle containing only aldehyde-terminated PEG-PLA (obtained earlier) and acetal-terminated PEG–PLA (10/90, w/w) in *N,N*-dimethylacetamide. Following this step, we performed dialysis against water for 24 h. We adjusted the solution to pH 5 by adding NaOH and dialyzed against water for 24 h for the removal of the salt. We concentrated the solution by evaporating at 50–60°C.

In vitro hydrogel formation

The solutions containing either a polymeric micelle (10 or 17 w/w%, pH 5, 0.25 mL) or polyallylamine (0.5–2.0 w/w%, pH 6–9 which was adjusted by HCl/NaOH, 0.25 mL) were mixed in a glass vial (length: 2 cm and inner diameter 1.6 mm) at 37°C. The hydrogel strength and the gelation time were then evaluated. The time period required for the magnetic stirring bar to stop stirring was defined as the gelation time of the mixed solution.[16] We observed the fluidity of the hydrogel from the top of the vial to the bottom by setting the vial in an inverted position after hydrogel formation. Using a coagulometer (Biomatic B10 model; Sarstedt, UK), we determined the gelation properties of the hydrogel by mixing the solutions containing either a polymeric micelle (10 or 17 w/w%, pH 5, 0.25 mL) or polyallylamine (0.5–2.0 w/w%, pH 6–9, 0.25 mL). We obtained the calibration curve by using a glycerine solution (60–90 w/w%) whose viscosity was determined via a viscosity meter VM-1G (Nikkato, Osaka, Japan).

In vivo hydrogel formation

Pentobarbital sodium (Nembutal™, Dainippon Pharmaceutical, Japan) was injected intraperitoneally into ddY mice. We performed celiotomy by creating an abdominal incision. By using tweezers to move the hydrogel, we evaluated the ability of the hydrogel to adhere to the peritoneum of mice. We used the following two methods to form the hydrogel—Method A: The solutions containing either a polymeric micelle (18 w/w%, pH 5) or polyallylamine (2.0 w/w%, at pH 9) were simultaneously applied to the peritoneum of mice. For this method, we used a two-pronged needle that consisted of two syringes and that is commonly used for the application of commercially available tissue-adhesive, namely, BOLHEAL™ (Kaketsuken, Japan) in order to mix two solutions. Method B: The solutions containing either a polymeric micelle (18 w/w%, pH 5) or polyallylamine (2.0 w/w%, pH 6) were mixed *in vitro* and were applied to the peritoneum of mice. Then an addition of sodium carbonate, wherein hematoxylin was solubilized (7.0 w/w%, pH 11.5), increased the pH. It is difficult to measure the final pH in Method B *in vivo*, since it was observed that the whole applied volume of a sodium carbonate solution (pH 11.5) was not used due to a low viscosity of this solution (most volume of the solution dispersed on the tissue without being used for an increase in pH of the more viscous solution of the polymeric micelle and the polyallylamine). We performed a control experiment by using commercially available fibrin glue, namely, Beriplast™ (Aventice Behring, Germany).

RESULTS AND DISCUSSION

In vitro hydrogel formation by a magnetic stirring

There still remains a clinical need for effective tissue-adhesive glues, even though numerous tissue-adhesive materials have been proposed and tested preclinically and clinically. One of the desired features of tissue-adhesive glues is reduced gelation time, that is, gelation within a few seconds. The gelation time and the hydrogel strength of our novel hydrogel are shown in Table I. The hydrogel was rapidly formed when the polymeric micelle solution and the polyallylamine solution were mixed under the experimental conditions with a few exceptions. The time required for hydrogel formation (2 s) was comparable to or shorter than that previously reported for other tissue-adhesive hydrogels. This property of the hydrogel is important from the viewpoint of its clinical applications. It is difficult to form a hydrogel on a tissue surface when the time required for *in vivo* hydrogel formation is long because the polymeric micelle solution and the polyallylamine solution gradually disperse before the hydrogel is completely formed.

We obtained the hydrogel by forming—in a pH-dependent manner—the Schiff base. No hydrogel formation was observed when the polyallylamine solution at pH 6 was used (entry 1), whereas hydrogel was formed when the pH of the polyallylamine solution was higher than 7 (entries 2–6) (entry codes are shown in the tables). The hydrogel was formed in ~2 s in the latter cases. However, there is a subtle difference in

TABLE I
Properties of the Tissue-Adhesive Hydrogel Formed *In Vitro*

Entry	Concentration of Polymeric Micelle (w/w%)	Polyallylamine			Hydrogel Strength[a]	Gelation Time (s)[b]
		Molecular Weight (g/mol)	Concentration (w/w%)	pH (−)		
1	10	150,000	1.0	6.0	−	−
2	10	150,000	1.0	7.0	+++	<2
3	10	150,000	1.0	7.5	+++	<2
4	10	150,000	1.0	8.0	+++	<2
5	10	150,000	1.0	8.5	+++	<2
6	10	150,000	1.0	9.0	+++	<2
7	10	150,000	2.0	8.0	+++	<2
8	10	150,000	0.5	8.0	+++	<2
9	10	60,000	1.0	8.0	++	<2
10	10	15,000	1.0	8.0	+	<2
11	10	5,000	1.0	8.0	−	−
12	17	150,000	1.0	8.0	+++	<2

[a]We observed the hydrogel's fluidity from the top to the bottom of the vial was observed by setting the vial in the inverted position after hydrogel formation (−, hydrogel was not formed; +, hydrogel rapidly moved to the bottom within 2 s; ++, hydrogel moved slowly; +++, hydrogel did not move).
[b]−, hydrogel was not formed.

each case: the hydrogel was gradually formed when the polyallylamine solution at pH 7 was used, whereas the gelation was slightly faster when the polyallylamine solutions at pH 8–9 were used. Schiff base formation ($R_1—NH_2 + CHO—R_2 \rightleftharpoons R_1—N=CH—R_2 + H_2O$) is faster at a slightly acidic pH: for instance, Schiff base formation between 5-formyluracil and 5-aminocytosine is faster at pH 5.8 than at pH 7.0.[17] However, because a primary amine obeys the equilibrium $R_1—NH_2 + H^+ \rightleftharpoons R_1—NH_3^+$, the concentration of reactive $R_1—NH_2$ thus increases as pH increases. Thus, there is an optimal pH for Schiff base formation. In our case, the hydrogel was rapidly formed when the polyallylamine solutions at pH 8 and 9 were used, whereas a white aggregate with a low gel strength was formed when the polyallylamine solution at a pH over 10 was used (data not shown). These findings indicate that the optimal pH for the formation of the Schiff base between polyallylamine and the aldehyde groups on the surface of a polymeric micelle is 8–9.

The hydrogel strength was greatly dependent on the molecular weight of polyallylamine. We evaluated hydrogel strength by observing the fluidity of the hydrogel from the top to the bottom of the vial by setting the vial in an inverted position. On the basis of the fluidity, the hydrogel strength was classified into four categories as follows: (+) hydrogel rapidly moved to the bottom within 2 s, (++) hydrogel moved slowly, (+++) hydrogel did not move, and (−) hydrogel was not formed. The hydrogel strength lowered as the molecular weight of the polyallylamine decreased (entries 4, 9–11). This outcome indicates that the main chain length of polyallylamine was an important factor in the regulation of a hydrogel strength. It become clear that when the molecular weight of polyallylamine was 150,000 and when the concentration of polyallylamine was 0.5–2.0 w/w%, the hydrogel strength was sufficiently high, thereby making the gel elastic (entries 2–8). The hydrogel did not move in the inverted vial when the concentration of the polymeric micelle was 17 w/w% (entry 12). We observed that, in this case, the gel strength was slightly higher than the gel strength that manifested itself when the concentration of the polymeric micelle was 10 w/w% (entry 4). Even in the former case, a gelation time was still short, and this finding indicates that the increase of the viscosity of a polymeric micelle solution did not influence the diffusion property of the polymeric micelle.

In vitro hydrogel formation by a coagulometer

We further evaluated the gelation properties by using a coagulometer that could detect the change in viscosity in a short time range (Table II), because the hydrogel formation that we induced by mixing the polymeric micelle solution and polyallylamine solution was rapid. A coagulometer can facilitate monitoring of the blood-clotting process by "tapping (not mixing)" a blood sample. Thus, for the application of the hydrogel *in vivo* in the next steps, a coagulometer-determined hydrogel gives rise to properties that are expected to be more useful than the properties that correspond to a hydrogel obtained via magnetic stirring (mentioned earlier). Figure 3 shows the typical time-course of the coagulometer-determined gelation (ca. 90 in the output value was the detection limit of the coagulometer). The solution showed the almost the same output value before the addition of a polymeric micelle solution (the solution was added at $t = 0$). However, once a polymeric micelle solution was added, the output value changed depending on the

TABLE II
Properties of the Tissue-Adhesive Hydrogel Formed *In Vitro* Determined by Coagulometer

Entry[a]	Concentration of Polymeric Micelle (w/w%)	Polyallylamine			Hydrogel Viscosity (mPa·s)	Time Required by the Hydrogel to Reach a Viscosity of 30 mPa·s
		Molecular Weight (g/mol)	Concentration (w/w%)	pH (–)		
2a	10	150,000	1.0	7.0	>40	3.0
3a	10	150,000	1.0	7.5	>40	2.0
4a	10	150,000	1.0	8.0	>40	2.0
5a	10	150,000	1.0	8.5	>40	2.0
6a	10	150,000	1.0	9.0	>40	1.7
7a	10	150,000	2.0	8.0	>40	1.5
8a	10	150,000	0.5	8.0	>40	3.3
9a	10	60,000	1.0	8.0	>40	1.4
10a	10	15,000	1.0	8.0	>40	1.6
11a	10	5,000	1.0	8.0	4	–[b]
12a	17	150,000	1.0	8.0	>40	1.3

[a] –, Entry numbers are consistent with those in Table I except an addition of "a". For example, entry 2a in Table II corresponds to entry 2 in Table I.
[b] –, hydrogel was not formed.

gelation property of the mixed solution obtained. Namely, the output value increased by a gelation (solid line in Fig. 3), whereas in the case when the hydrogel was not formed, the output value did not increase (dotted line in Fig. 3).

This coagulometer outputs the values in response to the resistance to the detection bar, which was induced by the change in the solution's viscosity. We thus determined the calibration curve by using a glycerine solution whose viscosity was already determined via a viscosity meter (Fig. 4). It is obvious that the upper detection limit of the coagulometer was 40 mPa·s in viscosity. Table II summarizes the gelation property of the mixed solution. The hydrogel showed almost the same viscosity in our experimental condition, except when the molecular weight of polyallylamine was low (entry 11a), indicating that the main chain should be sufficiently long to form a hydrogel. The gelation rate could be evaluated on the basis of the time required for the viscosity of the hydrogel to reach 30 mPa·s. The hydrogel formation was enhanced when either the pH of the polyallylamine solution was higher (a comparison of entries 3a–6a with entry 2a) or the concentration of the polyallylamine was higher (a comparison of entries 6a–7a with entry 8a). Although the gelation times, as evaluated according to the two methods, differed from each other owing to the difference in the gel-forming method (mixing or tapping), similar results were obtained (Tables I and II). The coagulometer-based evaluation clearly showed the gelation properties in a short time range that are important when the hydrogel is applied *in vivo*.

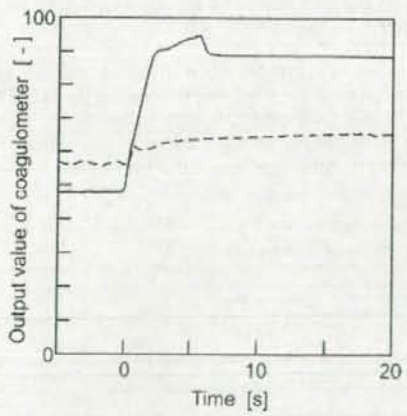

Figure 3. Typical time-course of the hydrogel determined by a coagulometer. The solid line shows the case when the hydrogel was formed (entry 4 in Table I), whereas the dotted line shows the case when the hydrogel was not formed (entry 11 in Table I).

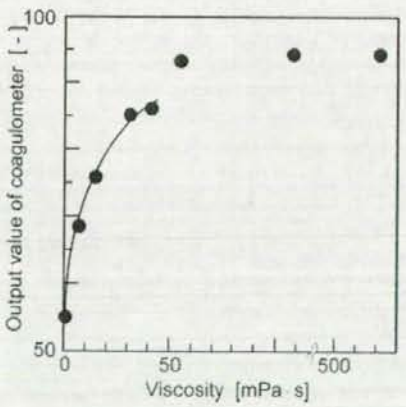

Figure 4. Calibration of coagulometer (output values of coagulometer were plotted against the viscosity of the solution).

Further optimization studies are currently being performed. As shown in Tables I and II, it is obvious that the formation of the Schiff base (depending on the pH) and the formation of the crosslinks (depending on the molecular weight and the concentration of the main chain-forming polymer and the concentration of the crosslinkable molecule) are important for the formation of the hydrogel proposed in this study.

In vivo hydrogel formation

We evaluated the hydrogel formation on the peritoneum of mice. The hydrogel was formed according to two methods. One method employed the simultaneous application of both the polymeric micelle and the polyallylamine solutions to the peritoneum of mice (Method A). The other method involved (1) the application of both the solution containing the polymeric micelle and polyallylamine to the peritoneum of mice and (2) the addition of sodium carbonate so that pH would increase (Method B). With Method A as well as Method B, the hydrogel was rapidly formed on the peritoneum of mice (Fig. 5, the hydrogel was slightly colored by hematoxylin for easy visualization in the latter case). The transparent and thin hydrogel adhered to a tissue surface.

We examined the effect that density of the aldehyde-terminated group had on the surface of the polymeric micelle. We used two types of polymeric micelles-one consisting of aldehyde (100 w/w%)-terminated PEG-PLA (entries 13 and 15) and the other consisting of aldehyde (10 w/w%)/acetal (90 w/w%)-terminated PEG-PLA (entries 14 and 16) (Table III). We performed a control experiment by using commercially available fibrin glue. We found that the hydrogel strength was sufficiently high, and that it therefore made the gel elastic. This was observed in all cases, independently of the density of the aldehyde-terminated group on the surface of the polymeric micelle. On the other hand, the adhesion strength of the hydrogel to the peritoneum of mice decreased as the density of the aldehyde-terminated group on the surface of the polymeric micelle decreased (entries 14 and 16). The currently available tissue-adhesive materials adhere to tissues because of the mechanical bonding provided by polymerized monomers, which penetrate the tissues in a soluble form during the polymerization ("anchor effect"). Although this is also true for the hydrogel pre-

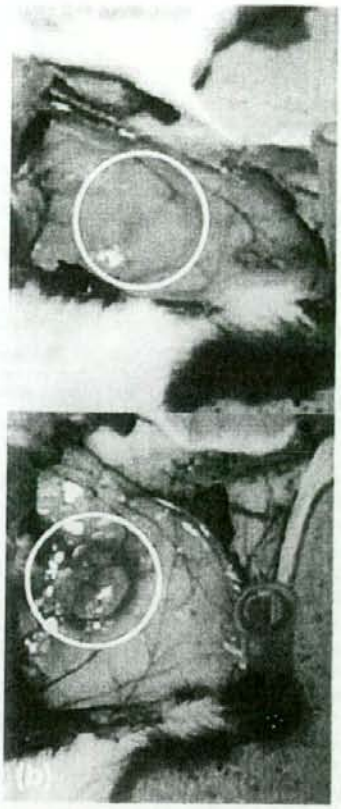

Figure 5. The hydrogel that adheres to the peritoneum of a mouse [(a) Method A and (b) Method B]. White circle shows the hydrogel formed.

TABLE III
Properties of the Tissue-Adhesive Hydrogel Formed *In Vivo*

	Polymeric Micelle		Polyallylamine					
Entry	Concentration (w/w%)	Aldehyde-Terminated Groups (w/w%)	Molecular Weight (g/mol)	Concentration (w/w%)	pH (−)	Method	Hydrogel Strength[a]	Adhesion Strength[b]
13	18	100	150,000	2.0	9.0	A	+++	+
14	18	10	150,000	2.0	9.0	A	+++	−
15	18	100	150,000	2.0	6.0	B	+++	+
16	18	10	150,000	2.0	6.0	B	+++	−

[a] We observed the hydrogel's fluidity from the top to the bottom of the vial was observed by setting the vial in the inverted position after hydrogel formation (keys are the same as shown in Table I).

[b] +, Adhesion strength was comparable to that of the fibrin glue; −, adhesion strength was weaker than that of the fibrin glue.

pared in this study, the additional tissue-adhesive mechanism based on a chemical bonding has another advantage. As shown in Table III, the gel adhesion strength was affected by the density of the aldehyde-terminated group on the surface of the polymeric micelle, even though the hydrogel strength was independent of the density. This result suggests that the hydrogel adheres to tissues according to two mechanisms: (1) the Schiff base formation between the aldehyde groups in the polymeric micelles and the amino groups that are present on the tissue surface and (2) the conventional anchor effect-that is, mechanical bonding enables the gel to fit into the uneven surface of tissues.

CONCLUSIONS

We successfully prepared a novel tissue-adhesive hydrogel by using a crosslinkable polymeric micelle. The incorporation of the crosslinkable polymeric micelle into the hydrogel could make the micelle a novel biomaterial. Two solutions containing either a polymeric micelle or polyallylamine formed a hydrogel *in vivo* and *in vitro* immediately after these two solutions were mixed. The hydrogel adhered to the peritoneum of mice.

The novel hydrogel prepared in this study has some interesting features. It has been reported that aldehydes with low molecular weights as crosslinkers are cytotoxic because of their high permeability into tissue, thereby allowing them to penetrate tissues. For this study, we used a macromolecular crosslinker that was expected to have a low permeability into tissue. The components of polymeric micelles (PEG and PLA) are known to be noncytotoxic and biocompatible. Our novel adhesive does not carry the risk of transmission of infectious contaminations, because it consists of only synthetic materials. Although an aldehyde-terminated polymeric micelle has been one of the useful functional carriers in drug delivery systems,[18] it is necessary that future research test the biocompatibility of the hydrogel in detail. The evaluation of other polyamines (e.g. poly(amino acid) and chitosan) is now underway, because polyallylamine, which was used in this study, may not be the best choice as an amine component for medical use. Although quantitative investigations concerning hydorogel properties are necessary in the future, the preliminary results obtained in the present study show that a hydrogel prepared through a crosslinkable polymeric micelle has the potential to address the need for novel adhesives.

References

1. Morikawa T. Tissue sealing. Am J Surg 2001;182:29S–35S.
2. MacGillivray TE. Fibrin sealants and glues. J Card Surg 2003; 18:480–485.
3. Czerny M, Verrel F, Weber H, Muller N, Kircheis L, Lang W, Steckmeier B, Trubel W. Collagen patch coated with fibrin glue components. Treatment of suture hole bleedings in vascular reconstruction. J Cardiovasc Surg 2000;41:553–557.
4. Turner AS, Parker D, Egbert B, Maroney M, Armstrong R, Powers N. Evaluation of a novel hemostatic device in an ovine parenchymal organ bleeding model of normal and impaired hemostasis. J Biomed Mater Res (Appl Biomater) 2002; 63:37–47.
5. Taguchi T, Saito H, Uchida Y, Sakane M, Kobayashi H, Kataoka K, Tanaka J. Bonding of soft tissues using a novel tissue adhesive consisting of a citric acid derivative and collagen. Mater Sci Eng C 2004;24:775–780.
6. Fukunaga S, Karck M, Harringer W, Cremer J, Rhein C, Haverich A. The use of gelatin–resorcin–formalin glue in acute aortic dissection type A. Eur J Cardiothorac Surg 1999;15:564–570.
7. Kumar A, Maartens NF, Kaye AH. Evaluation of the use of BioGlue in neurosurgical procedures. J Clin Neurosci 2003;10: 661–664.
8. Singer AJ, Thode HC. A review of the literature on octylcyanoacrylate tissue adhesive. Am J Surg 2004;187:238–248.
9. Ramakumar S, Roberts WW, Fugita OE, Colegrove P, Nicol TM, Jarrett TW, Kavoussi LR, Slepian MJ. Local hemostasis during laparoscopic partial nephrectomy using biodegradable hydrogels: Initial porcine results. J Endourol 2002;16: 489–494.
10. Nakayama Y, Matsuda T. Photocurable surgical tissue adhesive glues composed of photoreactive gelatin and poly(ethylene glycol) diacrylate. J Biomed Mater Res (Appl Biomater) 1999;48: 511–521.
11. Ferland R, Mulani D, Campbell PK. Evaluation of sprayable polyethylene glycol adhesion barrier in a porcine efficacy model. Hum Reprod 2001;16:2718–2723.
12. Wallace DG, Cruise GM, Rhee WM, Schroeder JA, Prior JJ, Ju J, Maroney M, Duronio J, Ngo MH, Estridge T, Coker GC. A tissue sealant based on reactive multifunctional polyethylene glycol. J Biomed Mater Res (Appl Biomater) 2001;58:545–555.
13. Kitamura K, Yasuoka R, Ohara M, Shimotsuma M, Hagiwara A, Yamane T, Yamaguchi T, Takahashi T. How safe are the xenogeneic hemostats?—Report of a case of severe systemic allergic reaction. Surg Today 1995;25:433–435.
14. Yokoyama M. Drug targeting with nano-sized carrier systems. J Artif Organs 2005;8:77–84.
15. Scholz C, Iijima M, Nagasaki Y, Kataoka K. A novel reactive polymeric micelle with aldehyde groups on its surface. Macromolecules 1995;28:7295–7297.
16. Otani Y, Tabata Y, Ikada Y. A new biological glue from gelatin and poly(L-glutamic acid). J Biomed Mater Res 1996;31:157–166.
17. Dohno C, Okamoto A, Saito I. Stable, specific, and reversible base pairing via Schiff base. J Am Chem Soc 2005;127:16681–16684.
18. Nagasaki Y, Okada T, Scholz C, Iijima M, Kato M, Kataoka K. The reactive polymeric micelle based on an aldehyde-ended poly(ethylene glycol)/poly(lactide) block copolymer. Macromolecules 1998;31:1473–1479.

Available online at www.sciencedirect.com
ScienceDirect
Journal of Controlled Release 114 (2006) 325–333
journal of controlled release
www.elsevier.com/locate/jconrel

A polymeric micelle MRI contrast agent with changeable relaxivity

Emiko Nakamura [a], Kimiko Makino [a], Teruo Okano [b], Tatsuhiro Yamamoto [c], Masayuki Yokoyama [c,*]

[a] Tokyo University of Science, Department of Pharmaceutics, 2641 Yamasaki, Noda, Chiba 278-8510, Japan
[b] Tokyo Women's Medical University, Institute of Advanced Biomedical Engineering and Science, Kawada-cho 8-1, Shinjuku-ku, Tokyo 162-8666, Japan
[c] Kanagawa Academy of Science and Technology, Yokoyama "Nano-medical polymers" project, KSP East 404, Sakado 3-2-1, Takatsu-ku, Kawasaki-shi, Kanagawa 213-0012, Japan

Received 24 March 2006; accepted 31 May 2006
Available online 15 June 2006

Abstract

Polymeric micelles were formed from cationic polymers (polyallylamine or protamine) and anionic block copolymers (poly(ethylene glycol)-*b*-poly(aspartic acid) derivative) that bound Gd ions providing high contrasts in Magnetic Resonance Imaging (MRI) by shortening the T_1 longitudinal relaxation time of protons of water. The Gd-binding block copolymer alone showed high relaxivity (T_1-shortening ability) values from 10 to 11 $mol^{-1}\ s^{-1}$, while the polymeric micelles exhibited low relaxivity values from 2.1 to 3.6 $mol^{-1}\ s^{-1}$. These findings point to the feasibility of a novel MRI contrast agent that selectively provides high contrasts at solid tumor sites owing to a dissociation of the micelle structures, while selective delivery to the tumor sites is achieved in the polymeric micelle form.

Keywords: MRI; Contrast agent; Polymeric micelle; Relaxivity; Targeting

1. Introduction

Magnetic resonance imaging (MRI) is one of the most useful methodologies in the field of diagnostic imaging, and its novel applications such as imaging of gene expression are actively studied [1]. This methodology is characterized by its high resolution of soft-tissues and by its non-exposure to radiation. So that the resolution and the sensitivity of MRI can be raised, a kind of medical agent is used. This is called an MRI contrast agent. Presently, approximately 30% of all MRI images are obtained using this type of contrast agent, and this use is on the increase [2]. Gd-DTPA (Gd-diethylenetriaminepentaacetate, its commercial product name is Magnevist) is the most commonly used MRI contrast agent that shortens the T_1 longitudinal relaxation time of protons of water and that increases the contrast of the image owing to the thus shortened relaxation time. However, this low molecular weight contrast agent has significant problems such as short half-life in blood and lack of specificity to target organs and tissues for diagnosis. Therefore, much of the contrast agent is administered to a patient before an image is taken, and this substantial agent injection is a heavy burden for patients. So that this problem can be resolved, many macromolecular carriers have been examined for increases in relaxivity and specificity. Studied carriers include poly(ethylene glycol) [3,4], dendrimers [5–8], dextrans [9,10], other polysaccharides [11,12], disulfide-based biodegradable synthetic polymers [13], PEG-grafted poly(L-lysine) [14], and conjugates of polymers and targeting moieties such as antibodies [15] and folates [16]. DTPA or another chelating unit was conjugated to these polymeric carriers. None of these, however, has accomplished increases both in relaxivity and in specificity. As a result of these concerns, no macromolecular contrast agent has been approved for clinical use. Alternatively, there are some attempts for the attainment of tumor-specific MRI contrast agents, and these attempts utilize pH [17,18] or enzymatic activity [19]. However, the pH of the tumor site may differ greatly from person to person. In the other system, an enzyme was used to change relaxivity through cleavage of a

* Corresponding author. Tel.: +81 43 819 2093; fax: +81 43 819 2095.
E-mail address: masajun@ksp.or.jp (M. Yokoyama).

0168-3659/$ - see front matter © 2006 Elsevier B.V. All rights reserved.
doi:10.1016/j.jconrel.2006.05.030

protecting moiety that inhibited water molecules' access to a Gd ion. However, the used enzyme was merely a model enzyme, not a tumor-specific enzyme. Therefore, neither methodology has reached a stage for clinical applications.

On the other hand, drug targeting is now attracting great attention as ideal and safe methods for chemotherapies. The polymeric micelle is one of the most attractive drug carriers used in the field of drug targeting [20–23]. Polymeric micelles consist of AB-type block copolymers that have hydrophobic and hydrophilic segments and have many therapeutic advantages such as high stability in blood and small particle size. In the previous research [24–26], it was found that polymeric micelles selectively accumulated at tumors through an enhancement of the vascular permeability of the tumor vasculature (enhanced permeability and retention effect: EPR effect [27,28]). Polymeric micelles containing Doxorubicin [29] and Taxol [30] in the core of the micelles are now in clinical tests. Selective delivery to the target tissue or organs is also very beneficial for the MRI diagnosis, as is the delivery of drugs. The methodology of drug targeting may be different from that of the targeting of the MRI contrast, as described below. Therefore, a new carrier design is an important key to the establishment of the most appropriate targeting system of the contrast agent.

For the drug targeting, an increase in a drug concentration at the targeted site is important. On the other hand, to have a large amount of drugs circulating in the bloodstream for a long time period is not considered a problem. Actually, the high drug concentration in the bloodstream is a prerequisite for the efficient delivery of a drug from the bloodstream to organs or tissues. Different from the drug targeting, a high concentration of MRI contrast agents circulating in the bloodstream causes a problem. A high concentration of the contrast agents in the vascular space creates a disadvantageous background, since blood is supplied both to the targeted tissues (or organs) and to the non-target ones. This is a possible reason for the fact that no highly tumor-specific image has been obtained, even in the most successful example of the contrast agent delivery specific to solid tumor sites [14]. From these considerations for an ideal MRI contrast agent, it is necessary not only to increase the signal intensity at the targeted site but also to lower the signal intensity in the vascular space. In order to accomplish this, we have tried to design a polymeric micelle-type MRI contrast agent that can change image contrasts between the target site and the vascular space, as shown in Fig. 1.

Various metals such as Gd, Fe, and Mn are used for MRI contrast agents [31]. Above all, the metal Gd is extensively used as a contrast agent for its strong paramagnetic effect. [32] Gd ions can function as an MRI contrast agent by interacting with water molecules near the Gd ions [2]. By these interactions, Gd ions enhance MRI contrasts by shortening the T_1 longitudinal relaxation times of protons of water. Therefore, if the Gd ions are in a hydrophobic circumstance, such as an inner core of a polymeric micelle, the T_1-shortening ability may be suppressed at a low level. Therefore, when a Gd-containing micelle circulates in the bloodstream stably, the signal intensity can be low. After the delivery of this micelle to tumor sites, the micelle structure gradually dissociates into single polymer chains. Once the micelle structure dissociates at the tumor sites, Gd in the core of the micelle can interact with water molecules, and consequently the MRI contrast becomes high. On the other hand, if the polymeric micelle structure dissociates in the bloodstream into a single polymer chain, the single polymer chain, which has a molecular weight lower than the critical molecular weight of the renal excretion (ca. 40,000), will be rapidly excreted in the urine. Therefore, the signal intensity of the vascular space remains low. In addition, if the micelle structure dissociates in the tumor vasculature, the dissociated chain can be retained in the tumor site for a long time owing to the poor lymphatic drainage at the tumor site. This retention phenomenon of polymers at the tumor site is one part of the EPR effect [27,28], which is an essential principle for the tumor targeting of polymers. As stated above, the polymeric micelle containing Gd in the core can achieve the tumor-specific imaging both by providing high signal intensity at solid tumor sites and by lowering blood signal intensity, as illustrated in Fig. 1. Additionally, a required dose for the MRI imaging can be reduced owing to this targeting effect. On the basis of this

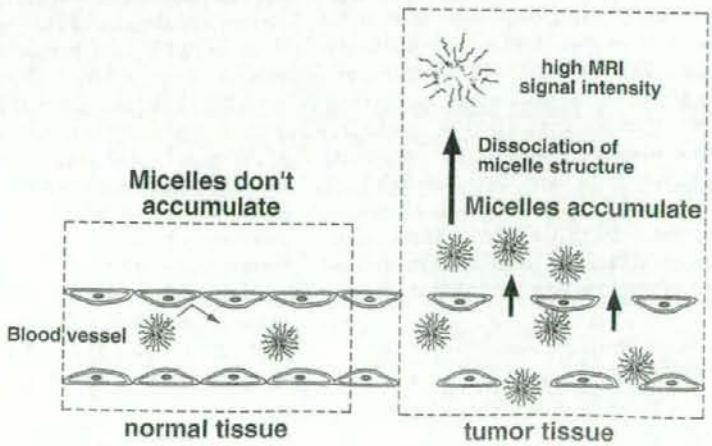

Fig. 1. Concept of polymeric micelle-type MRI contrast agent for tumor imaging.

perspective, we synthesized a novel polymeric micelle-type macromolecular contrast agent and evaluated its micelle-forming behavior and its T_1-shortening ability relative to the MRI contrast agent.

2. Materials and methods

2.1. Materials

Poly(ethylene glycol)-*b*-poly(β-benzyl L-aspartate) (PEG-PBLA, **1**) was synthesized according to the reported method [33]. *N*-Boc-ethylenediamine (*N*-Boc-ED), diethylenetriamine-pentaaceticacid anhydride (DTPA ba), and protamine sulfate were purchased from Sigma-Aldrich Japan, Tokyo, Japan. Gadolinium chloride hexahydrate ($GdCl_3 \cdot 6H_2O$) was purchased from Wako Pure Chemical Industries, Ltd., Tokyo, Japan. Polyallylamine (average M.W. 15,000) was a kind gift from Nitto Boseki Co., Ltd., Tokyo, Japan. Gd-DTPA (Magnevist™) was purchased from Schering Japan, Osaka, Japan. The other chemicals were of reagent grade and were used as purchased.

2.2. Synthesis of PEG-P(Asp) block copolymer

A synthesis route of the Gd-binding block copolymer is shown in Fig. 2. Poly(ethylene glycol)-*b*-poly(aspartic acid) (PEG-P(Asp), **2**) block copolymer was prepared through alkali hydrolysis of poly(ethylene glycol)-*b*-poly(β-benzyl L-aspartate) (PEG-PBLA, **1**) block polymer [33]. The composition of PEG-P(Asp) was determined through an ^{1}H-NMR measurement carried out in D_2O at 23 °C, as shown in Fig. 3(a). The number of Asp units was found to be 44 from the peak intensity ratio between the methylene protons of the PEG block (3.5 ppm) and the methylene protons of the P(Asp) block (2.7 ppm). The obtained block copolymer that was composed of 114 ethylene oxide units and 44 Asp units on the average was coded as PEG-P (Asp) 114–44. It was known that alkali hydrolysis transformed the α-amide bonds of the BLA units into β-amide bonds [34]. The content of the β-amide bonds was measured through the peak intensity ratio of the methine protons of the α-amide (4.7 ppm) and the β-amide (4.5 ppm) of an ^{1}H-NMR spectrum in D_2O at pD 9.2 [35]. For PEG-P(Asp) 114–44, the β-amide content out of all the amide bonds turned out to be 66%.

2.3. Introduction of primary amino groups to PEG-P(Asp) block copolymer

PEG-P(Asp) 114–44 (**2**, 0.400 g) was dissolved in 2.5 ml DMSO. 1-Ethyl-3-(3-dimethylaminopropyl)carbodiimide hydrochloride (EDC HCl, 84.4 mg) and *N*-Boc-ethylenediamine (*N*-Boc-ED, 75.8 mg) were dissolved in 2.6 ml and 0.43 ml of DMSO, respectively. Molar ratios both of EDC HCl and of *N*-Boc-ED were adjusted to 1/4 to the carboxyl groups of the P (Asp) chain. The PEG-P(Asp) solution was mixed with the EDC HCl and *N*-Boc-ED solutions, and the reaction mixture was stirred at room temperature for 4 h. Then, the reaction mixture was dialyzed against distilled water for a few days (M.W. cut off= 1000) and lyophilized. The number of *N*-Boc-EDs bound to one PEG-P(Asp) block copolymer chain was calculated according to the methylene protons of the PEG (3.5 ppm) and to the methyl protons of the Boc units (1.4 ppm), as shown in Fig. 3(b). Considerably parge peaks at 1.7 ppm and 1.0 ppm were revealed to be of residual EDC derivatives. These two impurity peaks disappeared after the deprotection procedure of the *N*-Boc group, as shown in Fig. 3(c). The *N*-Boc-ED unit number per PEG-P(Asp) 114–44 chain was 9.1. From this value, the reaction yield was calculated and found to be high, about 82%. For other runs, the number of the bound N-Boc-ED unit was controlled by the molar ratios both of EDC HCl and of *N*-Boc-ED to the carboxyl groups of the P(Asp) chain. Deprotection of the Boc units was carried out using

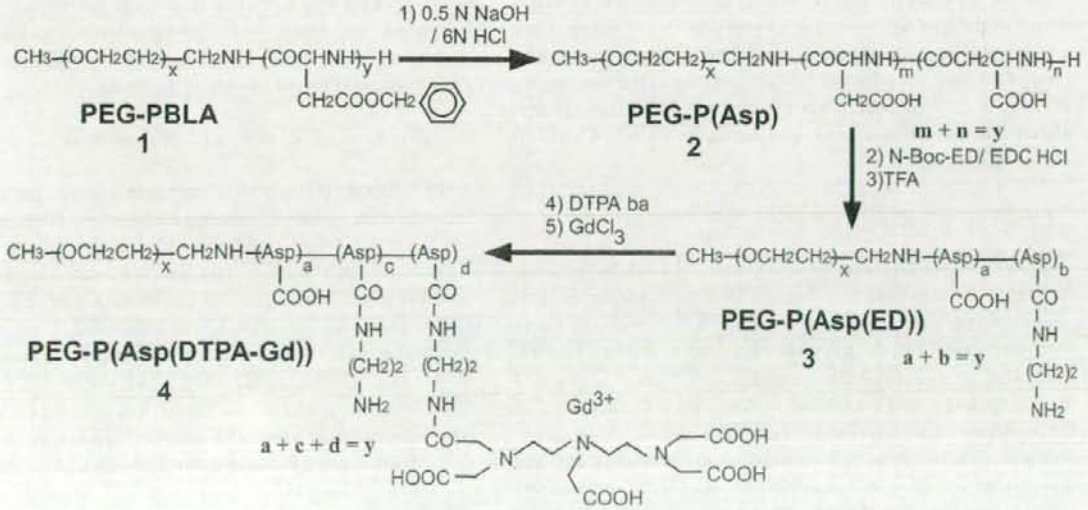

Fig. 2. Synthesis of PEG-P(Asp(DTPA-Gd)).

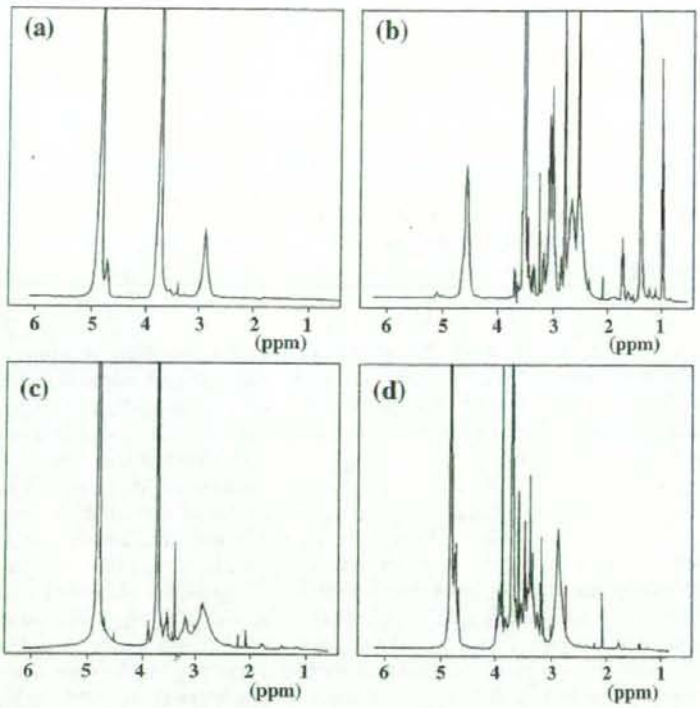

Fig. 3. ^{1}H-NMR spectra of block copolymers. (a) PEG-P(Asp) 114-44, (b) *N*-Boc-ED-conjugated PEG-P(Asp) 114–44, (c) PEG-P(Asp(ED)) 114–44(N9.1), (d) PEG-P(Asp(DTPA)) 114–44(N9.1–D5.4). D_2O was used as solvent for (a), (c), and (d), while ^{6}D-DMSO was used for (b).

TFA. The obtained block copolymer (200 mg) was dissolved in 4 ml TFA in an iced bath, and the solution was stirred for 1 h. Then, the TFA was evaporated, and 5 ml of H_2O was added, followed by dialysis against MeOH overnight. After evaporation of the MeOH, 5 ml of H_2O was added, and the solution was lyophilized. Disappearance of a methyl peak in the Boc group (1.4 ppm) confirmed the deprotection of the Boc group, as shown in Fig. 3(c). This synthesized block copolymer, which had 9.1 units of ED was coded as PEG-P(Asp(ED)) 114–44(N9.1) (**3**).

2.4. Conjugation of DTPA to block copolymer

PEG-P(Asp(ED)) block copolymer 114–44(N 9.1) (**3**, 100 mg) was dissolved in 5.2 ml of DMSO. Diethylenetriaminepentaacetic acid bisanhydride (DTPA ba, 173 mg) and triethylamine (TEA, 17 μl) were dissolved in 3 ml of DMSO. The molar ratio of DTPA ba was adjusted to 5 to the ED group of the P(Asp) chain, and the ratio of TEA was 1.5 to the ED group of the P(Asp) chain. The PEG-P(Asp(ED)) solution was mixed with the DTPA ba and TEA solutions, and the reaction mixture was stirred for 24 h at room temperature. Then, the reaction mixture was dialyzed against distilled water for a few days and lyophilized. The obtained polymer that had the DTPA groups was coded as PEG-P(Asp(DTPA)). The composition of PEG-P(Asp(DTPA)) was determined through an ^{1}H-NMR measurement in D_2O. The number of bound DTPA was calculated from the peak intensity ratio of the methylene protons of PEG (3.5 ppm) and the methylene protons of DTPA (3.9 ppm), as shown in Fig. 3(d). The number of the bound DTPA units per polymer chain was 6.7. From this value, the reaction yield was calculated, and it was 74%. This synthesized block copolymer containing 9.1 units of ED and 6.7 units of DTPA was coded as PEG-P(Asp(DTPA)) 114–44(N9.1–D6.7).

2.5. Chelation of Gd ions to block copolymer

PEG-P(Asp(DTPA)) (10.2 mg) was dissolved in 1 ml H_2O. One milliliter of $GdCl_3$ solution containing 2.0 mol equivalent Gd ion to the DTPA units was added to the polymer solution. After a 10 min stirring, this solution was dialyzed against distilled water overnight. The Gd-binding number of 114–44 (N9.1–D6.7) was calculated from Inductively Coupled Plasma spectrometry (ICP), and it turned out to be 15. This polymer was coded as PEG-P(Asp(DTPA-Gd)) 114–44(N9.1–D6.7–Gd15) (**4**). For some preparations, EDTA was added to the polymer solution before dialysis. A molar ratio of EDTA was adjusted to 0.2–2.0 with respect to the carboxyl groups of the P(Asp) chain.

2.6. Preparation of polymeric micelles from block copolymer and cationic polymer

PEG-P(Asp-(DTPA-Gd)) 114–44(N9.1–D8.9–Gd7.3) (**4**, 5.2 mg) was dissolved in 0.5 M NaCl aqueous solution

(1.2 ml), and its pH was adjusted to 7.0±0.2. Poly(allylamine) (PAA) 0.1 w/w% solution (pH 7±0.2, 0.5 M NaCl) was added to the PEG-P(Asp(DTPA-Gd)) 114–44(N9.1–D8.9–Gd7.3) solution, and the mixture was stirred for 10 min, followed by dialysis against distilled water overnight. When protamine was used as the cationic polymer on behalf of the PAA, the protamine and the block copolymer were dissolved in 10 mM NaCl aqueous solution. We prepared the polymeric micelles by mixing these two solutions in a manner identical to that used for the PAA.

2.7. Measurements

We measured the content of the Gd ion through Inductively Coupled Plasma (ICP) and used an SPS 7800 apparatus (Seiko Instruments Inc., Tokyo, Japan). Micelle-forming behaviors were evaluated through gel-permeation chromatography (GPC), which involved the use of a TSK Gel G3000PWXL column (Tosoh, Tokyo, Japan) at 40 °C. The eluent was distilled water, and the flow rate was 1.0 ml/min. The polymer concentration ranged from 0.3 to 0.5 mg/ml, and detection was made through RI and UV (240 nm) detectors. Dynamic light scattering (DLS) measurements were carried out through the use of a DLS-700 apparatus (Otsuka Electronics, Tokyo, Japan) at 25 °C. ^{1}H-NMR measurements were carried out through a Varian Inova 400 NMR spectrometer by the use of D_2O or ^{6}D-DMSO as solvent. To evaluate a function as an MRI contrast agent, the T_1 longitudinal relaxation time was measured through a Varian Inova 400 NMR spectrometer. Polymer or micelle solutions in a mixture of 20% D_2O and 80% H_2O were measured in three concentrations at 23 °C. Relaxivity was calculated through the formula described below [36].

$$1/T_1\mathrm{obs} = 1/T_1\mathrm{d} + R_1 \cdot [P]$$

where $[P]$ is a concentration of a paramagnetic species (in this study, $[P]$ is [Gd]), T_1d is relaxation time in the absence of the paramagnetic species, T_1obs is relaxation time in the presence of the paramagnetic species, and R_1 is specific relaxivity. The correlation coefficient r^2 values of the fitted line obtained from three plots were 0.990 and higher in all measurements.

3. Results and discussion

3.1. Synthesis

Poly(ethylene glycol)-*b*-poly(aspartic acid) (PEG-P(Asp), **2**) block copolymer was obtained through alkali hydrolysis of a poly (ethylene glycol)-*b*-poly(β-benzyl L-aspartate) (PEG-PBLA, **1**) block copolymer. Two PEG-P(Asp) block copolymers were obtained. One had, as its average number of ethylene glycol units, 114 (this corresponds to M.W. 5000) and, as its average number of Asp units, 44. This was coded as 114–44. The other block copolymer was 273–26. The P(Asp) chain of these block copolymers had two kinds of amide bonds, α-amide and β-amide. The β-amide content was found to be 66% out of the total amide bonds of the P(Asp) chain for PEG-P(Asp) 114–44. For 273–26, this content was 73%. Compositions of the block copolymers' binding to Gd through the DTPA chelating group are summarized in Table 1.

The introduction of *N*-Boc-ethylenediamine (*N*-Boc-ED) to the P(Asp) chain was efficient and exhibited high reaction yields of the *N*-Boc-ED group in a range from 58% to 84% for various compositions. Deprotection of the *N*-Boc-ED group was done with TFA, and this deprotection reaction proceeded completely, as confirmed by the disappearance of a methyl peak attributable to the Boc units in the ^{1}H-NMR spectra, as shown in Fig. 3(c). Then, diethylenetriaminepentaacetic acid anhydride (DTPA ba) was reacted with the primary amino group of the ED group of the PEG-P(Asp(ED)) (**3**) block copolymer. The DTPA group was found to be bound to 74% of the ED group for the 114–44(N9.1) block copolymer. This means that 26% of the ED groups remained unreacted even at a high DTPA/ED molar ratio, such as 5 in the feed.

The introduction of Gd ions to DTPA was carried out through the addition of $GdCl_3$ to the block copolymer in distilled water, and the number of Gd ions per one polymer chain was measured through an Inductively Coupled Plasma (ICP) method. When an excess number of Gd atoms (Gd/DTPA molar ratio was 2.0) was added to the PEG-P(Asp(DTPA)) solution, the number of bound Gd ions was found to be larger (15) than that of the introduced DTPA (6.7), as shown by run 1 in Table 1. The obtained solution

Table 1
Composition of PEG-P(Asp(DTPA-Gd))

Run	PEG-P(Asp(DTPA-Gd)) code	Unit number of block (molecular weight)		Addition of Gd[a]	Addition of EDTA[b]	Number of bound moiety per polymer chain			Molecular weight[c]
		PEG[d]	P(Asp)[c]			Ethylene diamine	DTPA	Gd	
1	114–44(N9.1–D6.7–Gd15)	114 (5000)	44 (5060)	2.0	0	9.1	6.7	15[e]	15,500
2	114–44(N9.1–D6.7–Gd3.3)	114 (5000)	44 (5060)	2.0	1.0	9.1	6.7	3.3	13,400
3	114–44(N16–D8.9–Gd5.9)	114 (5000)	44 (5060)	2.0	1.5	16	8.9	5.9	15,400
4	114–44(N16–D8.9–Gd7.3)	114 (5000)	44 (5060)	2.0	1.0	16	8.9	7.3	15,600
5	273–26(N10–D5.4–Gd10)	273 (12,000)	26 (2990)	2.0	0	10	5.4	10[e]	19,200
6	273–26(N7.4–D5.1–Gd3.2)	273 (12,000)	26 (2990)	1.5	0.2	7.4	5.1	3.2	17,900

[a] Molar ratio to DTPA moiety.
[b] Molar ratio to carboxyl group of P(Asp) block.
[c] Determined by ^{1}H-NMR.
[d] Determined by GPC.
[e] Larger Gd numbers than the DTPA numbers indicate that Gd ions were bound to unmodified aspartic acid residues as well as the DTPA moiety, as explained in text.

Table 2
Formation of polymeric micelles from block copolymer and polyallylamine (PAA)

Polymer(s)	Charge ratio[a]	GPC elution volume (ml)[b]	Average diameter[c] (nm)
PAA[d] alone	–	10.0	Not done
114–44(N16) alone	–	6.2	Not detected
114–44(N16–D8.9–Gd5.9)+PAA	1:1.0	3.3	Not done
114–44(N16–D8.9–Gd7.3)+PAA	1:2.0	5.6	31±14

[a] –COOH of the P(Asp)/–NH_2 of PAA.
[b] Column: TSK gel G3000 PwXL(Tosoh, Japan).
[c] Weight–weighted average±standard deviation determined by dynamic light scattering.
[d] PAA; polyallylamine, average molecular weight 15,000.

of this run 1 was cloudy. This result indicates that the carboxyl groups of unmodified aspartic acid residues contributed to the chelation of the Gd ions. It is expected that Gd ions were chelated by plural unmodified Asp groups, and consequently that block copolymers were chemically bound through bridge formation at the Gd ions. In fact, the number of the unmodified aspartic acid residue (35=44−9.1) was more than four-fold value of the excess Gd number (33.2≈4×(15−6.7)). So that this contribution of the unmodified Asp groups would be avoided, EDTA was added to the mixture of both the PEG-P(Asp(DTPA)) and the Gd ions before dialysis. The stability constant of the EDTA-Gd was considered to be larger than that of the carboxyl group of the P (Asp) chain-Gd. Lu et al. reported the use of EDTA to clear off an excess amount of Gd ions bound to the carboxyl groups of poly (glutamic acid) [37]. Through ICP, they confirmed the clearance of Gd ions. In fact, by adding EDTA, the number of Gd ions bound to PEG-P(Asp(DTPA)) decreased from 15 to 3.3, as shown by run 2 in Table 1, and the obtained solution was clear. However, the number of Gd ions bound to the synthesized polymer was considerably lower than the number of DTPA units. In runs 3 and 4, the block copolymer, which possessed the same chain lengths both of the PEG block and P(Asp) block but possessed a larger number of the DTPA moiety, was used. The number of the bound Gd ions to the block copolymer was found to de dependent on a quantity of the added EDTA; the larger EDTA addition resulted in the smaller number of the bound Gd ions. In run 4, the Gd-binding block copolymer was obtained with a considerably high chelation ratio of the DTPA moiety (7.3 Gd ions bound to 8.9 DTPA moieties). For the block copolymer 273–26 that had a longer PEG block and a shorter P(Asp) block than 114–44, the same behavior concerning the clear-off effect of EDTA was observed, and a transparent solution of the Gd-binding block copolymer was successfully obtained in run 6.

3.2. Preparation and evaluation of polymeric micelles

Polymeric micelles were formed through the mixing of PEG-P (Asp(DTPA-Gd)) and polycation, PAA, or protamine, followed by dialysis against distilled water. The formation of micelles was confirmed by a light-scattering phenomenon (Tyndall phenomenon), gel-permeation chromatography (GPC), and dynamic light scattering (DLS). The Tyndall phenomenon was observed on a visible light path of a laser pointer. This phenomenon was not observed for the PEG-P(Asp(DTPA-Gd)) solution or the PAA solution. Then, the polymeric micelle solution was analyzed through GPC. Results are shown in Table 2. The elution volumes of PEG-P(Asp(ED)) 114–44(N16) and of the PAA solution were 6.2 ml and 10 ml, respectively. The elution volumes of the mixtures ranged from 3.3 to 5.6 ml, indicating that elution volume decreased when PEG-P(Asp(DTPA-Gd)) was mixed with the polycations. These results indicated that PEG-P(Asp-(DTPA-Gd)) associated with the polycations in a structure such as a polymeric micelle. Then, dynamic light scattering measurement was carried out. No particle was detected in the solutions of either the PAA or the PEG-P(Asp(DTPA-Gd)). In contrast, small particles were detected in the mixture of PEG-P(Asp(DTPA-Gd)) and a polycation, and their weight-weighted size was 31 nm for 114–44(N16–D8.9–Gd7.3) and PAA. All these data indicated that association, regarding for example polymeric micelles, was formed in the mixture of PEG-P (Asp(DTPA-Gd)) and the polycation. When the PEG-P(Asp (DTPA-Gd)) and the PAA were mixed in 10 mM NaCl, the same association was obtained, and that was confirmed through GPC, DLS, and observation of the Tyndall phenomenon. Polymeric micelles were also found to form when PEG-P(Asp(DTPA-Gd)) and protamine were mixed in 10 mM NaCl.

When PAA was used as a polycation, the micelle solution contained both small particles with the weight-weighted average of 27 nm and large particles with 119 nm in the diameter, as shown in Table 3. From these average diameter values, it is considered that the small particles correspond to a polymeric micelle structure possessing a single inner core and that the larger particles correspond to secondary associates of these polymeric micelles. On the other hand, in the two protamine-included micelle cases, only monodispersed particle distributions with the average diameters larger than 100 nm were detected, and DLS spectra showed considerably narrow diameter distributions that were seen by small

Table 3
Micelle diameter from PEG-P(Asp(DTPA-Gd)) and polyallylamine (PAA) or protamine

PEG-P(Asp(DTPA-Gd))	Polycation	Charge ratio –COOH/–NH_2	Diameter[a] (nm)
273–26(N10–D5.4–Gd10)	PAA	1:2.0	27±4 and 119±20
273–26(N10–D5.4–Gd10)	Protamine	1:2.0	142±53
273–26(N7.4–D5.1–Gd3.2)	Protamine	1:2.0	292±76

[a] The weight–weighted average±standard deviation.